Digest Journal of Nanomaterials and Biostructures Vol. 19, No. 4, October-December 2024, p.1975-1985

Affordable excellence: unveiling the potential of graphitic carbon-based counter electrodes for high-performance dye-sensitized solar cells

N. Sharma[a], M. Mittal[a], A. Saini[b], P. Singh[c], A. Kumari[d], A. Kumar[e], P. K. Jangra[f], P. Tiwari[g], S. Choudhary[h], A. S. Verma[i,j,*]

[a]*Department of Physics, Dhanauri P.G. College, Dhanauri, Haridwar, Uttarakhand, 247667, India*

[b]*Department of Chemistry, Dhanauri P.G. College, Dhanauri, Haridwar, Uttarakhand, 247667, India*

[c]*Department of Electronics and Communication Engineering, KIET Group of Institutions, Ghaziabad 201206, India*

[d]*Department of Physics, S. V. College, Raja Mahendra Pratap Singh State University, Aligarh, 202140, India*

[e]*Department of Physics, Government College for Women, Badhra, Charkhi Dadri, Haryana 127308 (India)*

[f]*Department of Chemistry, Government College for Women, Badhra, Charkhi Dadri, Haryana 127308, India*

[g]*Department of Physical Sciences, Banasthali Vidyapith, Rajasthan, 304022, India*

[h]*Department of Physics, Constituent Government Degree College, Richha Baheri, Bareilly, 243201, India*

[i]*Division of Research and Innovation, School of Applied and Life Sciences, Uttaranchal University, Dehradun, 248007, India*

[j]*University Centre for Research & Development, Department of Physics, Chandigarh University, Mohali, Punjab, 140413, India*

Dye-Sensitized Solar Cells (DSSCs) have emerged as a promising alternative energy technology due to their minimal material requirements and straightforward production process, enabling efficient performance even under low-light conditions. Traditionally, high-performance DSSCs utilize platinum as the counter electrode. However, the high cost of platinum necessitates the development of more affordable counter electrodes that can match or surpass platinum-based counter electrodes (CEs) in conversion efficiency. This study investigates the synthesis and application of various cost-effective counter electrodes, including candle flame carbon soot, pencil lead graphite, and CS-coated PLG, in high-efficiency DSSCs. For comparison, a platinum-based counter electrode is used as a benchmark. The working electrode comprises TiO_2 on Fluorine-Doped Tin Oxide substrates. The DSSCs fabricated with counter electrodes such as PLG, CS, and CS-coated PLG exhibit efficiencies of approximately 6.2%, 3.5%, and 8.5%, respectively, compared to 10.8% for the Pt-based counter electrode. Reduced series resistance contributes to an improved Fill Factor and increased conversion efficiency. Furthermore, impedance spectroscopy reveals higher capacitance at the CE/electrolyte interface, enhancing charge collection efficiency and electron lifetime. Thus, the potential for significant improvement in conversion efficiency makes low-cost PLG and carbon-based electrodes a highly attractive alternative to Pt-based electrodes.

(Received June 26, 2024; Accepted December 20, 2024)

Keywords: DSSC solar cell, Counter electrodes; UV-visible spectra, I-V curve

* Corresponding author: ajay_phy@rediffmail.com
https://doi.org/10.15251/DJNB.2024.194.1975

1. Introduction

Development of green and renewable energy is one of the possible ways to solve the problem of global pollution and reduce the consumption of fossil fuels to ultimately decrease the greenhouse effect. A great deal of work has been devoted to the progressive development of various green and renewable energy. One of them is the photovoltaic (PV) system, which has gained significant development over the years. The worries of energy deprivation and environmental pollution have both paved the way for significant enthusiasm in solar cell research [1-2]. DSSCs have gained tremendous attention because they are cost-effective, easy to fabricate, and nontoxic, making them an attractive alternative to first-generation solar cells [3]. However, their solar efficiency is still low, so researchers are focusing on ways to enhance the performance of DSSCs in general by trying different materials for the working electrode (WE) and counter electrode (CE) [4].

The DSSCs have been fabricated by making use of different kinds of semiconductor materials like titanium dioxide (TiO_2), zinc oxide (ZnO), and tin oxide (SnO_2). Among these, TiO_2 is considered the most reliable semiconductor material, and hence it has shown 10.4% efficiency, achieved with the cells using black dye and TiO_2 as the photo-anode [5]. Huang et al [6] have synthesized mesoporous TiO_2 spheres through sol-gel and solvo-thermal. The DSSCs prepared had a maximum efficiency of 10.3% compared to those based on the commercial TiO_2 nanoparticles and improved to 11.4% upon using $TiCl_4$ post-treatment to enhance the mesoporous TiO_2 spheres [6]. Platinum (Pt) has also been popular as a CE material in DSSC coatings. Although Pt is costly and less abundant, it remains to be used because of its outstanding catalytic and conduction performance [7]. Pt promotes fast electron transfer in DSSCs, and this is very important for enhancing the overall performance of DSSCs. However, its cost is also the biggest disadvantage of using Pt. Therefore, researchers and firms have considered other materials for CEs in DSSC applications. The counter electrode in DSSCs plays a significant role in catalyzing redox reactions, accepting electrons, and transferring them to the electrolyte for further synthesis. The CE and low internal resistance with high catalytic activity are significant for yielding tri-iodide to iodide, thus enhancing the fill factor (FF) [9]. Therefore, alternatives to Pt for CEs in DSSCs must be addressed from both economic and other aspects. Appropriate CE materials in DSSCs should have low charge-transfer resistance, optimal thickness, extensive surface area, considerable light reflectance, great electrochemical stability in the electrolyte, and large current density exchange [12-13].

Several alternatives to Pt have been investigated, including carbon soot, graphite, activated carbon, conductive carbon black, and graphene [14]. These materials have high catalytic activity, are easily available, iodine corrosion resistance, and cost-effective. Due to high conductivity, carbon-based materials and polymers have received significant research attention as CEs [6]. PLG CEs are one of the varieties investigated, due to their low price, environmentally friendly nature, and high potential to enhance efficiency. However, there are numerous problems in these materials, such as the processes used are inconsistent, due to which they cannot be used as CE materials. The most common problem with PEDOT-based CEs is their high price in comparison with Pt, while PPy-based CEs are cheaper but deliver slightly lower efficiency than PEDOT. PLG and carbon derived from candle flames show high surface area and good conductivity [16]. More interestingly, the coated carbon soot on PLG gives an even higher surface area and delivers high efficiency. In the present work, we have fabricated CEs using Pt by replacing materials like pencil lead graphite, carbon soot, and their composite to replace and achieved high efficiency. The present work demonstrates the potential of using a noble-metal-free and cost-effective strategy by using PLG and carbon soot and its combination toward the development of high-efficiency DSSCs.

2. Materials and methods

Herein, we have used a transparent titania paste with 22 nm particles, especially an opaque film colloidal paste from Sigma Aldrich. The material utilized was conductive glass coated with fluorine-doped tin oxide (FTO). The synthetic dye employed was di-tetrabutyl-ammonium cis- (N719), sourced from Sigma Aldrich. For the electrodes, materials included Pt paste from Sigma

Aldrich, carbon derived from a candle flame, and graphite obtained from pencil lead. The redox iodide electrolyte required for the process was likewise procured from Sigma Aldrich.

3. Counter electrode preparation

First, the FTO substrates were thoroughly cleaned in an ultrasonic bath, undergoing 15-minute cycles in deionized water, acetone, and 2-propanol. After the cleaning process, the substrates were treated in a UV-ozone system for 15-20 minutes to ensure proper surface cleanliness and activation. The fabrication of counter electrodes involved several methods, as detailed below.

A. Pt-Coated CE

- The Pt-coated CE was made with the doctor blade procedure.
- Sigma Aldrich's industrial Pt paste was applied to the FTO substrate.
- The coated substrate was then sintered at 450°C for 30 minutes in a furnace to form a crack-free layer.

B. Carbon CE

- The carbon CE was formed by putting an FTO substrate to a candle flame in a back-and-forth motion.
- This process deposited carbon soot onto the conductive glass, forming the carbon layer.

C. Graphite CE

- The graphite CE was formed by rubbing a pencil over the glass's conducting surface.
- This simple procedure effectively coated the FTO substrate with graphite.

4. Working electrode preparation

The TiO_2 commercial paste was deposited on pre-cleaned FTO substrates using the doctor-blade method, forming a mesoporous TiO_2 network over an area of approximately 0.25 cm^2. The deposited TiO_2 layer was then annealed at 450°C for 30 minutes in a heating furnace.

The TiO_2 layer serves multiple functions:

- Enhancing the adhesion of TiO_2 nanoparticles to the FTO substrate.
- Providing a high TiO_2/FTO contact area, beneficial for electron transport.
- Reducing electron recombination by minimizing contact between the electrolyte and the FTO substrate surface.

After annealing, the coated FTO substrate was immersed in an ethanol solution containing 0.5 mM N719 dye for 24 hours in the dark at room temperature. This step allowed the dye molecules to adsorb onto the TiO_2 surface. Excess dye was removed with a cotton swab, and the substrate was air-dried for 5-10 minutes.

5. Fabrication of DSSC

The DSSC was assembled by creating a sandwich-like structure, where the dye-absorbed working electrode and the CE were placed together and held securely with a binder clip. The electrolyte solution was then introduced between the electrodes using a dropper, completing the DSSC device, as depicted in Figure 1 (a).

6. Operational principle

The photo-anode of a DSSC absorbs incoming light energy, causing dye electrons to transition from their ground state to a higher energy level. Due to this energy difference, the energised electrons are injected into the conduction band of a semiconductor material, typically TiO_2, thereby oxidizing the dye. These injected electrons move between TiO_2 particles and diffuse through the conductive oxide layer to the CE via the external circuit. At the counter electrode, the electrons reduce tri-iodide ions (I3-) to iodide ions (I-), which in turn regenerate the dye by donating electrons back to it. The iodide ions are then oxidized to form tri-iodide ions, and this cycle repeats as the tri-iodide ions diffuse back to the counter electrode to be reduced again to iodide ions.

The fundamental operation of a DSSC involves the following process:

- When light hits the dye, an electron is excited from the ground state to the excited state.
- This electron's energy is used to traverse the semiconducting oxide layers.
- The expelled electron travels to the transparent conducting electrodes and through the load, completing the external circuit.
- The dye is reduced by regaining an electron from the electrolyte, maintaining a closed loop.

DSSCs function based on two major reactions that need to be minimized for maximum efficiency:

- Recombination of the electrons in the conduction band with the oxidized dye.
- Recombination of conduction band electrons with iodine within the electrolyte.

7. Electron transfer in DSSC

The process of electron transfer in DSSCs gives rise to many chemical processes in what is depicted in figure 2 (b). This picture, in a nutshell, represents the main steps of the electron transfer mechanism that takes place in the DSSC, namely, the path of electrons from the absorbed incident light energy of dye molecules to injection into the semiconductor material, passing through the conductive oxide layer, to finally get regenerated at the counter electrode. Such processes play a crucial role in producing electrical energy in DSSCs and explaining the operation of DSSCs.

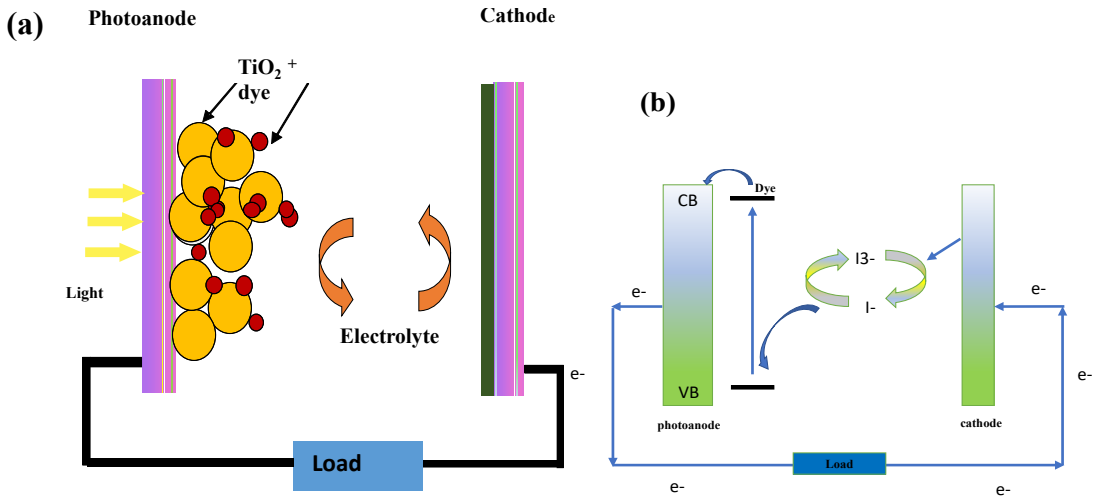

Fig. 1. (a) Schematic diagram and (b) electron transfer mechanism of DSSC.

8. Result and discussion

8.1. Surface morphology analysis:

Figure 2 depicts the surface morphology of CEs made of Pt, PLG, carbon shot, or a mixture of PLG and carbon shoot.

(a) Pt-based CE: The morphology of the Pt-based CE (Fig. 2a) reveals uniformly distributed small non-spherical particles. This structure is typical of Pt coatings and is known for its efficient catalytic activity.

(b) Candle flame carbon CE: The surface morphology of the candle flame carbon CE (Fig. 2b) shows an uneven distribution of carbon on the FTO substrate, appearing slightly porous. This porous character may influence the catalytic activity of the electrode.

(c) Pencil graphite (PLG) CE: In Fig. 2c, the pencil graphite particles appear elliptical and evenly distributed. However, the individual PLG particles are not sufficient to achieve optimal film quality.

(d) Carbon shoot over PLG: In Fig. 2d, the carbon shoot is a network to which PLG adheres, forming a cluster-like structure. This arrangement increases the surface area of the film, thus catalytic activity. However, adding carbon shoots over PLG causes the PLG particles to agglomerate into a bulk structure where even the graphite particles can hardly be identified.

These results highlight the effect of carbon shoot on PLG, stating that carbon shoot promotes contact among particles of graphite and hence enhances the quality of the film. In addition, the high carbon surface area of over PLG accounts for the catalytic activity of the counter electrodes. This research sheds light on the importance of morphology in optimizing the performance of DSSCs.

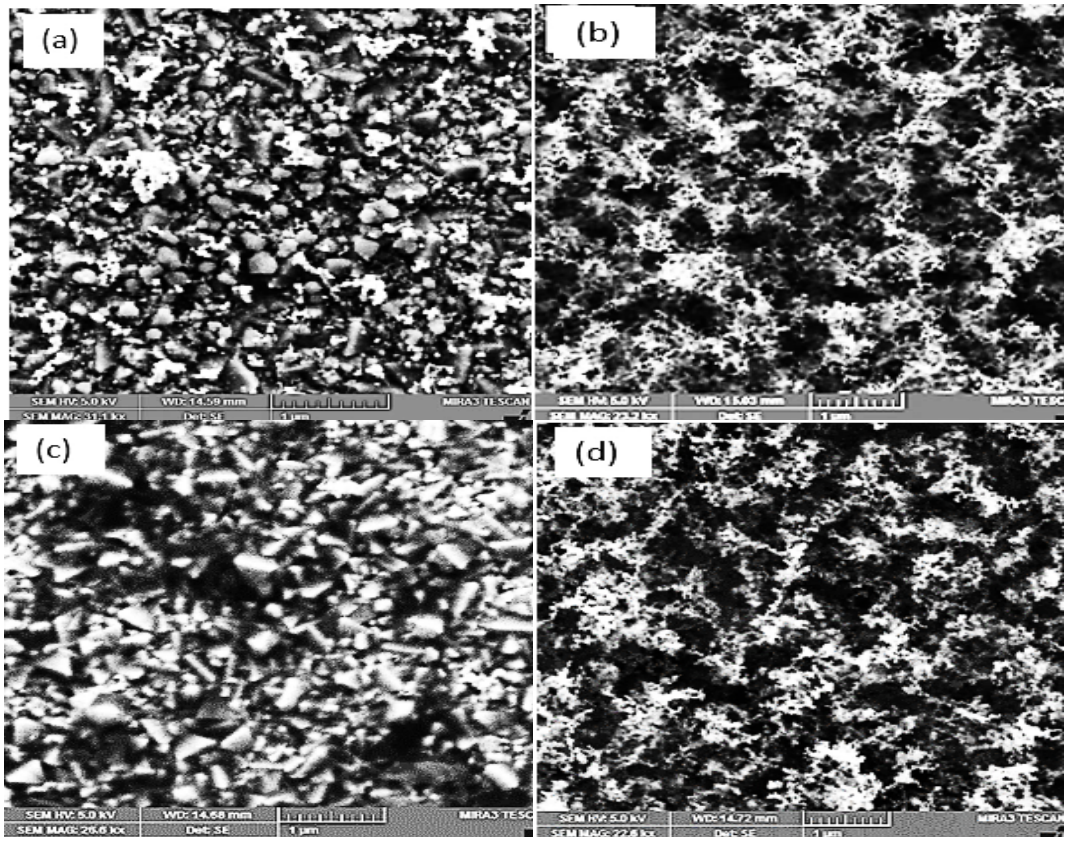

Fig. 2. FESEM images of CEs based on (a) platinum (b) carbon shoot (c) pencil lead graphite (PLG) and (d) carbon shoot over PLG.

8.2. Absorption study

Figure 3 depicts the absorption spectra of the N719 solution a very important sensitizer for light absorption in the blue and red regions of the visible spectrum. The absorption spectrum of the N719 solution reflects a significant increase in UV-Vis absorption in the 350–600 nm range [18]. The peak absorption levels at 388 and 536 nm are particularly notable, as they are dominated by broadband. These peaks are typically associated with a Metal-to-Ligand Charge-Transfer (MLCT) transition, in which an electron is transferred from Ruthenium (Ru) to one of the bipyridine ligands. A strong absorption peak at 311 nm indicates an electronic transition between the π-$\pi*$ orbitals of the dcbpyH ligands [19]. The broad absorption spectrum of the N719 solution enhances the capability of the solar spectrum to produce a predominant photocurrent. This absorption behaviour is critical to efficient light harvesting in DSSCs and contributes to their overall performance.

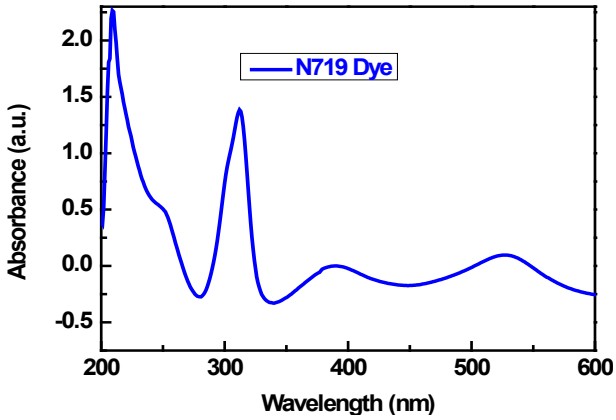

Fig. 3. Absorption Spectra of N719 dye solution.

8.3. Current-voltage characteristics

I-V characteristics have been presented in figure 4. During illumination, the following key variables define the power conversion efficiency of DSSCs: short-circuit current, J_{sc}; open-circuit voltage, V_{oc}; and Fill Factor. The J_{sc} is directly proportional to the photoelectrical performance of dye-loaded TiO_2 and the electro-catalytic activity on the counter electrode. The larger J_{sc} means the more effective light absorption and electron generation in the cell.

FF stands for the fill factor, which reflects how effective the cell is in translating the available power into electrical power. High FF values indicate good extraction of charge carriers and minimal losses in the cell.

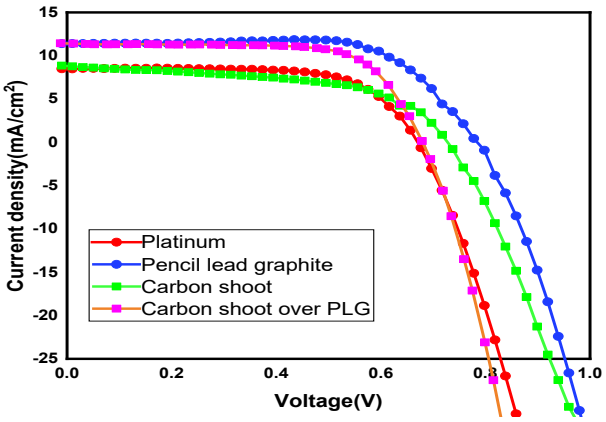

Fig. 4. Current-voltage curve for DSSC using different counter electrodes recorded at room temperature under AM 1.5 G illumination condition.

As shown in Table 1 and Fig. 4, the DSSCs with a pencil graphite CE, candle shoot, and carbon shoot over PLG CEs have the highest V_{oc}, J_{sc}, and FF values. In fact, with the carbon shoot over PLG used as the CE, the largest efficiency achieved is 8.5%, which thus indicates that cell performance is significantly increased when compared to other combinations. This indicates that using the carbon shot and PLG as a counter electrode enhances the efficiency and overall performance of the DSSC.

Table 1. Photovoltaic parameters of DSSCs constructed with different counter electrodes under AM 1.5 G illumination conditions.

Devices with Different CE	V_{oc} in (V)	J_{sc} (mA/cm^2)	FF	PCE (%)
Pt	0.66±0.03	23.6±1.7	65.2±7.4	10.2±0.7
PLG	0.66±0.11	12.0±1.21	71.5±3.4	5.8±0.5
CS	0.61±0.11	10.8±2.7	49.1±11.5	3.18±0.5
CS over PLG	0.66±0.017	17.08±1.08	71.6±3.21	8.17±0.44

Measurements were taken for five samples of each type of DSSC. The photovoltaic parameters shown in Table 1, demonstrate that the carbon-based CEs such as pencil graphite and candle flame and their combination can be better alternatives of Pt CE. Carbon material-based DSSCs have high FF similar to the Pt-based devices and their V_{oc} are very close to Pt CE-based cells. The carbon shoot has slightly low V_{oc}, which is probably due to a low charge recombination rate and the carbon shoot adheres weakly to the FTO, resulting in few cracks in the film. As a result, the DSSCs employing the corresponding CE resulting slightly less surface area and less charge transfer on that surface which may be a reason for a low value of η as compared to PLG and other CEs. However, carbon shoot over PLG enhances the formation of film and influences the performance of DSSCs. As shown in Table 1, the DSSC composed of carbon over PLG-based CE shows high J_{sc} which is due to better electron transport and low recombination that ensures a long electron lifetime.

8.4. Impedance analysis

Impedance measurements were carried out to know the variation in I-V performance at open circuit voltage. Using Z-View software, the equivalent circuit consists of series resistance (R_s), recombination resistance (R_{rec}), and chemical capacitance (CPE) [20]. Figure 5 shows the Nyquist plot of the impedance results from DSSCs, and Table 2 shows the R_s and R_{rec} values from the fitted data. The critical parameters are R_s and R_{rec} which describe the flow of electrons on the counter electrode at the time of reduction of tri-iodide [21]. The results from Table 2 infer that the carbon shoots have a lesser R_s value of 30.88Ω which shows reduced losses on the interface of CE and electrolyte and efficiency of 3.5%. However, it was found that the decline in FF and J_{sc} of the carbon shot is due to the increased internal resistance of the device [22]. This internal resistance arises due to the process of charge transfer between CEs, the sheet resistance (R_s) of the substrate, electron transfer in the interface of TiO_2/dye/electrolyte, and the transport of ions inside the electrolyte. The DSSC based on carbon shoot and pencil graphite CE has improved electron lifetime of 0.0230 sec and 0.0131 sec [23]. The lower R_s and high R_{rec} (24.35 Ω and 4070.65 Ω) indicate that the CE is made of carbon shoot (CS) over PLG and gives rise to a reduction in dark current and shows an improved V_{oc} and J_{sc} that affect the PCE of the device. The result obtained is in tandem with the fact that counter electrodes based on carbon, graphite, and its combination are reasonably comparable performance of Pt-based CE [24]. The charge collection efficiency (η_{cc}) represents the collection of injected electrons from the surface conduction band (CB) of TiO_2 at the FTO substrate. It relies on the ratio of charge transport to charge recombination, which can be expressed as $\eta_{cc} = (1 + R_s/R_{rec})^{-1}$ [2]. Achieving a better-performing cell necessitates a high charge collection efficiency. Electron transport (τ_t) is derived from $\tau_t = C_p * R_s$, while electron lifetime (τ_n) is given by $\tau_n = C_p * R_{rec}$.

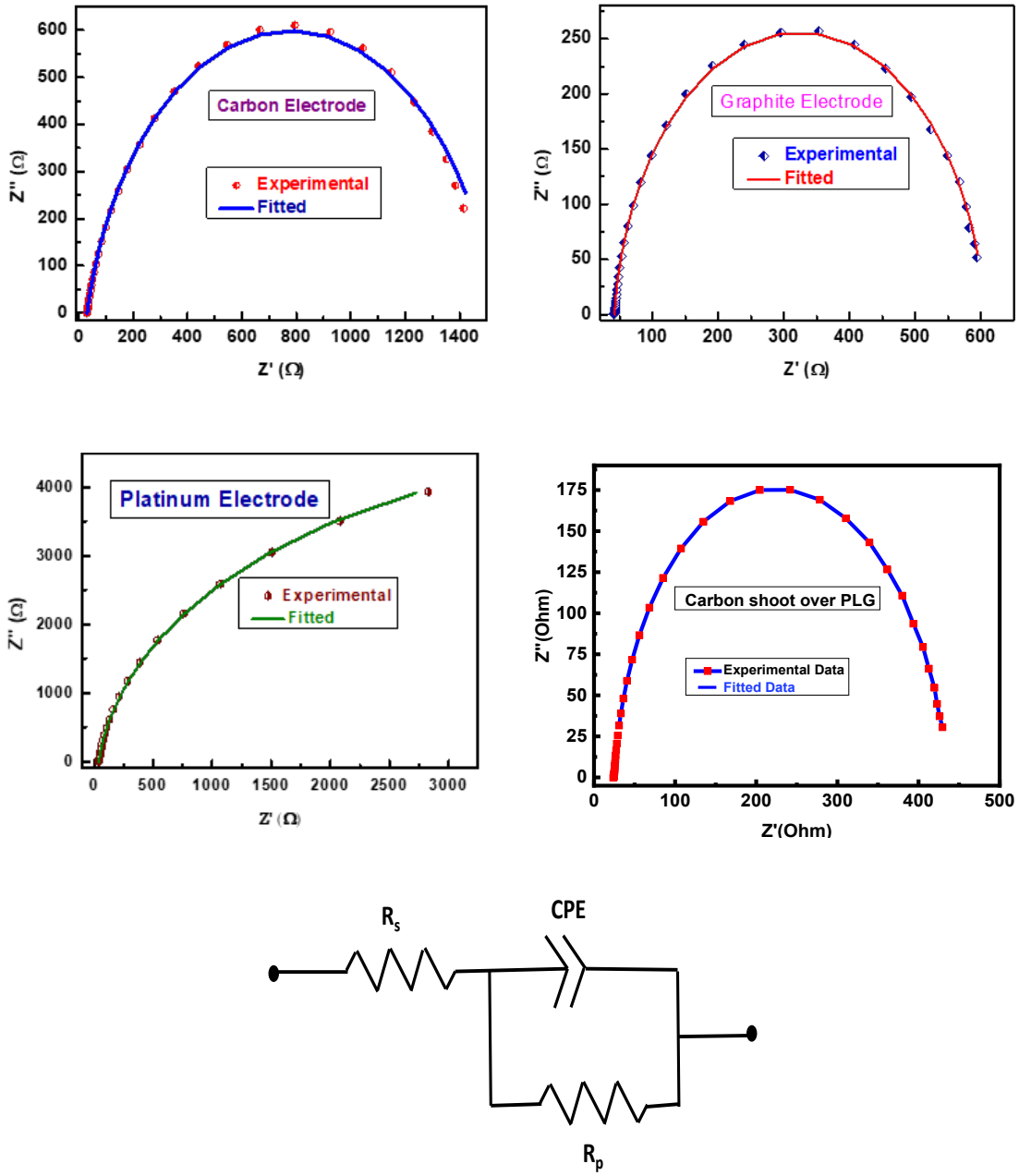

Fig. 5. Impedance spectra for DSSC based on different counter electrodes.

The significant increase in electron lifetime observed in carbon shoot may be attributed to a notable rise in capacitance ($\tau_n = C_p * R_{rec}$) at the CE/electrolyte interface. Carbon shoot exhibits a low series resistance (R_s) of 30.88Ω, implying a good electron lifetime of 0.0230 seconds and a high charge collection efficiency of up to 0.9798 seconds, showcasing significantly improved device performance [25].

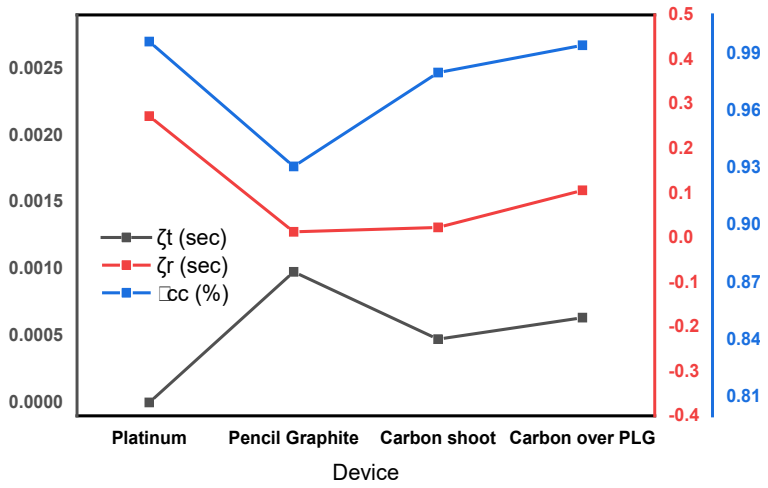

Fig. 6. Electron life time, electron transport time and charge collection efficiency of DSSC based on different CEs.

However, DSSCs based on PLG demonstrate slightly poorer electron lifetime and charge collection efficiency compared to carbon shoot CE-based cells, possibly due to high series resistance. Results are presented in figure 6. Carbon shoot exhibits very low series resistance (24.35 Ω) and a long electron lifetime of 0.1061 seconds due to minimal electron recombination with oxidized species of the electrolyte and a significant increase in capacitance (C_p) at the CE/electrolyte interface [26]. Consequently, a high charge collection efficiency of 0.9941 is achieved by reducing electron recombination, leading to enhanced cell performance. These results closely approach those of Pt CE, indicating an electron lifetime of 0.2727 seconds and a charge collection efficiency of 0.9960 [27].

Table 2. Parameters of Impedance for DSSCs based on different CEs.

Devices with different CE	**R_s(Ω)**	**R_{rec}(Ω)**	**CPE parameters**		**Capacitance (C_P) (μF)**	**τ_n(Sec)**	**τ_t (Sec)**	**η_{cc}**
			Q_o	**n**				
Pt	38.76	9601.7	3.07×10^{-5}	0.94	2.839×10^{-5}	0.2727	0.001×10^{-4}	0.9960
Pencil graphite	42.04	563.81	3.15×10^{-5}	0.93	2.325×10^{-5}	0.0131	9.777×10^{-4}	0.9306
CS	30.88	1499.7	2.7×10^{-5}	0.85	1.533×10^{-5}	0.0230	4.734×10^{-4}	0.9798
CS over PLG	24.35	4070.65	3.19×10^{-5}	0.91	2.606×10^{-5}	0.1061	6.347×10^{-4}	0.9941

9. Conclusions

The performance of the devices was evaluated based on their absorption response across the entire visible region, and the utilization of different types of counter electrodes yielded a significant performance improvement. As an alternative to Pt electrodes, various carbon-based electrodes were explored to enhance overall efficiency. The electrical properties and performance of carbon shoot, PLG, and carbon shoot over PLG, as discussed earlier, indicate their commendable catalytic performance.

Scanning Electron Microscopy SEM images revealed the porous nature of carbon and PLG-based counter electrodes, influencing the cell efficiency. Additionally, carbon shoot over graphite exhibited an increased surface area, contributing to the reduction of tri-iodide species. DSSCs prepared with graphitic carbon-based counter electrodes demonstrated a maximum efficiency of 8.5%, accompanied by a V_{oc} of 0.67 V, comparable to the performance of Pt CE.

EIS parameters provided insights into the enhanced efficiency, attributing it to improved charge carrier transfer at the electrolyte/counter electrode interface and reduced charge recombination. This capability has a positive impact on electron lifetime and charge collection efficiency, contributing to the overall success of the graphitic carbon-based counter electrodes in DSSCs.

References

[1] J. Chaudhary, R. Gautam, S. Choudhary, A. S. Verma, European Physical Journal Applied Physics 88 (2019) 30101; https://doi.org/10.1051/epjap/2019190023
[2] S. Chaudhary, S.K. Gupta, C.M.S. Negi, Mater Sci Semicond Process 109 (2020) 104916; https://doi.org/10.1016/j.mssp.2020.104916
[3] D. Kharkwal, N. Sharma, S. K. Gupta, C. M. S. Negi, Solar Energy 230 (2021) 1133; https://doi.org/10.1016/j.solener.2021.11.037
[4] J. Chaudhary, S. K. Gupta, A. S. Verma, C. M. S. Negi, J. Materials Science 55 (2020) 4345; https://doi.org/10.1007/s10853-019-04308-8
[5] M. K. Nazeeruddin, P. Pechy, T. Renouard, S. M. Zakeeruddin, R. Humphry-Baker, P. Comte, P. Liska, L. Cevey, E. Costa, V. Shklover, L. Spiccia, J. American Chemical Society 123 (2001) 1613; https://doi.org/10.1021/ja003299u
[6] Y. Huang, H. Wu, Q. Yu, J. Wang, C. Yu, J. Wang, S. Gao, S. Jiao, X. Zhang, P. Wang, ACS Sustainable Chemistry & Engineering 6 (2018) 3411; https://doi.org/10.1021/acssuschemeng.7b03626
[7] Z. Shi, K. Deng, L. Li, Scientific Reports 5 (2015) 9317; https://doi.org/10.1038/srep09317
[8] S. Kavitha, M. Lakshmi, Materials Today: Proceedings 92 (2023) 1544; https://doi.org/10.1016/j.matpr.2023.06.027
[9] G. Calogero, P. Calandra, A. Irrera, A. Sinopoli, I. Citro, G. Di Marco, Energy & Environmental Science 4 (2011) 1838; https://doi.org/10.1039/C0EE00463D
[10] R. Kumar, V. Sahajwalla, P. Bhargava, Nanoscale Advances 1 (2019) 3192; https://doi.org/10.1039/C9NA00206E
[11] S. Gullace, F. Nastasi, F. Puntoriero, S. Trusso, G. Calogero, Applied Surface Science 506 (2020) 144690; https://doi.org/10.1016/j.apsusc.2019.144690
[12] R. H. Althomali, S. I. S. Al-Hawary, A. Gehlot, M. T. Qasim, B. Abdullaeva, I. B. Sapaev, I. H. Al-Kharsan, A. Alsalamy, J. Physics and Chemistry of Solids 182 (2023) 111597; https://doi.org/10.1016/j.jpcs.2023.111597
[13] N. A. Al-Rawashdeh, B. A. Albiss, H. I. Moath, IOP Conference Series: Materials Science and Engineering 305 (2018) 012019; https://doi.org/10.1088/1757-899X/305/1/012019
[14] S. Rafique, I. Rashid, R. Sharif, Scientific Reports 11 (2021) 14830; https://doi.org/10.1038/s41598-021-94404-0
[15] G. Dwivedi, G. Munjal, A. N. Bhaskarwar, A. Chaudhary, Inorganic Chemistry Communications 135 (2022) 109087; https://doi.org/10.1016/j.inoche.2021.109087
[16] G. Yue, J. Wu, Y. Xiao, J. Lin, M. Huang, L. Fan, Y. Yao, Chinese Science Bulletin 58 (2013) 559; https://doi.org/10.1007/s11434-012-5352-3
[17] A. I. Rafieh, P. Ekanayake, H. Nakajima, A. H. Mahadi, M. Abu, M. F. Don, and C. M. Lim, J. Electronic Materials 50 (2021) 5788; https://doi.org/10.1007/s11664-021-09121-1
[18] D. M. Niedzwiedzki, Physical Chemistry Chemical Physics 23 (2021) 6182; https://doi.org/10.1039/D0CP06629J
[19] M. R. Elmorsy, F. H. Abdelhamed, S. A. Badawy, E. Abdel-Latif, A. A. Abdel-Shafi, M. A. Ismail, Scientific Reports 13 (2023) 13825; https://doi.org/10.1038/s41598-023-40830-1
[20] S. M. Faraz, M. Mazhar, W. Shah, H. Noor, Z. H. Awan, M. H. Sayyad, Physica B: Condensed Matter 602 (2021) 412567; https://doi.org/10.1016/j.physb.2020.412567
[21] W. Shah, R.W. Khwaja, S. M. Faraz, Z. H. Awan, M. H. Sayyad, Engineering Proceedings 46 (2023) 31; https://doi.org/10.3390/engproc2023046031
[22] M. Hosseinnezhad, M. Ghahari, G. Mobarhan, M. Fathi, A. Palevicius, V. Nutalapati, G. Janusas, S. Nasiri, Micromachines 14 (2023) 2161; https://doi.org/10.3390/mi14122161

[23] N. Sharma, C. M. S. Negi, M. Sharma, A. S. Verma, S. K. Gupta, Optical Materials 95 (2019) 109273; https://doi.org/10.1016/j.optmat.2019.109273
[24] N. Sharma, C. M. S. Negi, A. S. Verma, S. K. Gupta, J. Electronic Materials 47 (2018) 7023; https://doi.org/10.1007/s11664-018-6629-3
[25] S. Rudra, H. W. Seo, S. Sarker, D. M. Kim, J. Industrial and Engineering Chemistry 97 (2021) 574; https://doi.org/10.1016/j.jiec.2021.03.010
[26] D. Devadiga, M. Selvakumar, D. Devadiga, S. Paramasivam, T. N. Ahipa, P. Shetty, S. S. Kumar, J. Materials Science 58 (2023) 5718; https://doi.org/10.1007/s10853-023-08376-9
[27] E. Von Hauff, D. Klotz, J. Materials Chemistry C 10 (2022) 742; https://doi.org/10.1039/D1TC04727B